EXTENSION OF THE i-CRS OPERATOR TO CONVERTED WAVES

A. Bauer, B. Schwarz, C. Vanelle, and D. Gajewski

email: *alexander.bauer@zmaw.de*

keywords: *i-CRS, traveltimes, parameter estimation, converted waves, multi-parameter stacking*

ABSTRACT

Multi-parameter stacking for converted waves is important for seismic imaging because shear waves can carry additional information about the subsurface. In order to avoid acquisition problems associated with SS-surveys, PS-converted waves can be investigated instead. Recently, a non-hyperbolic traveltime expression, the implicit Common Reflection Surface (i-CRS) has been introduced. Since it treats the down- and up-going rays separately, i-CRS highly favors an extension to asymmetric settings. In this paper, we introduce two parameterizations of i-CRS for converted waves and examine their accuracy with synthetic data for different reflector curvatures and varying degrees of inhomogeneity. In addition, we present the results of a sensitivity study of the new operator. The results show that the two i-CRS expressions are superior to a hyperbolic operator. Moreover, we found that a five parameter expression leads to better results than an according three parameter expression for all examples investigated in this work.

INTRODUCTION

Shear waves play an important role in seismic imaging, because they can carry information about the subsurface that might not be provided by P-waves. For monotypic waves, i.e., PP or SS, multi-parameter stacking has become very important in applied seismics during the past decade, because stacking in both midpoint and half-offset direction allows for better results than classical stacking methods like the CMP stack. In order to avoid acquisition problems associated with SS-surveys, PS-converted waves can be investigated instead. Accordingly, multi-parameter stacking of PS-converted waves with a hyperbolic Common Reflection Surface (CRS, Müller, 1999) type operator has been suggested by Bergler et al. (2002).

In order to exploit the full potential of multi-parameter stacking, a highly accurate description of traveltime moveout is required. Common traveltime formulations like the CRS operator (Müller, 1999; Bergler et al., 2002) describe the traveltime moveout in a hyperbolic form, which has been shown by several authors (see, e.g., Vanelle et al., 2010) to be less accurate for highly-curved reflectors, and, in particular, diffractions. Therefore, it is reasonable to describe the traveltime in a non-hyperbolic form. Vanelle et al. (2011a) recently introduced a new stacking operator called implicit Common Reflection Surface (i-CRS). It was derived by searching the reflection point on a circle by Fermat's principle of least time. This leads to an implicit traveltime description depending on the reflection angle on the circle, which can be applied in a recursive fashion.

In this paper, we investigate the i-CRS operator for the case of converted waves as suggested by Vanelle et al. (2011a) and introduce two new parameterizations in terms of the widely-used CRS attributes (Hubral, 1983) adapted from Schwarz (2011). One formulation is based on the three CRS attributes, while the second one uses five instead of three optimization parameters, additionally incorporating the velocities of the down- and up-going rays, respectively. With these new operators, we perform several numerical studies on simple generic models in order to examine their accuracy and their ability to estimate the optimization parameters. The results are compared to those obtained by a simplified hyperbolic CRS operator for converted waves that implies a constant ratio of the P- and S-wave velocities (Vanelle et al., 2011b).

THEORY

Simplified CRS for converted waves

The CRS traveltime expression introduced by Bergler et al. (2002) has five parameters. Vanelle et al. (2011b) derived a simplified CRS operator with three parameters for converted waves under the assumption of a constant velocity ratio $\gamma = v_1/v_2$. In this special case, the paths of the down- and up-going zero-offset rays coincide. It has the advantage that the original CRS parameters, α, R_N, R_{NIP}, which describe a one-way process, can be used. In midpoint and half-offset coordinates, the simplified CRS operator reads:

$$\begin{aligned} t^2_{hyp}(\Delta x_m, h) = &\left(t_0 + \frac{2\sin\alpha}{v^+}\Delta x_m - \frac{2\sin\alpha}{v^-}h\right)^2 \\ &+ 2t_0\cos^2\alpha\left(\frac{\Delta x_m^2}{v^+R_N} + \frac{h^2}{v^+R_{NIP}}\right) \\ &- 2t_0\cos^2\alpha\left(\frac{(R_N - R_{NIP})}{R_N R_{NIP}}\frac{v^+h^2}{(v^-)^2} + \frac{2\Delta x_m h}{v^- R_N}\right). \end{aligned} \quad (1)$$

The abbreviations v^+ and v^-, respectively, denote:

$$\frac{2}{v^\pm} = \frac{1}{v_1} \pm \frac{1}{v_2}. \quad (2)$$

Indices 1 and 2 denote the down-going and up-going velocities, respectively. The velocity v^+ is the harmonic mean of the velocities v_1 and v_2. In the case of PS conversion we have $v_1 = v_P$ and $v_2 = v_S$. For monotypic waves, i.e., $v_1 = v_2 = v^+ = v^0$ and $1/v^- = 0$, the formula reduces to the monotypic CRS traveltime.

Derivation of the new operator

In areas with complex geology, the description of moveout by a hyperbola is not valid anymore. Therefore, the implicit CRS stacking operator (i-CRS) was introduced by Vanelle et al. (2010) for monotypic waves in isotropic media. It was extended by Vanelle et al. (2011a) to account for anisotropy and converted waves. In this section, we summarize their derivation before introducing two new parameterizations.

The operator is based on the idea of finding the reflection point on a circular reflector by applying Fermat's principle of least time. Using the Pythagorean theorem, it is possible to derive a formula for the reflection traveltime in a homogeneous medium consisting of two ray paths for the down- and up-going ray, respectively. Parameterizing the reflection point on the circle by its angle θ leads to the following traveltime description,

$$t = \frac{1}{v_1}\sqrt{(x_1 - x_c - R\sin\theta)^2 + (H - R\cos\theta)^2} + \frac{1}{v_2}\sqrt{(x_2 - x_c - R\sin\theta)^2 + (H - R\cos\theta)^2}, \quad (3)$$

where x_1 and x_2 denote the source and receiver coordinates, respectively. The parameters x_c, H, R describe the center and the radius of the circle.

In order to find the ray that needs the least time to travel from source to receiver, the traveltime function has to be minimized. This implies that $\partial t/\partial\theta = 0$ must hold. Calculating the derivative of t with respect to θ for the case of an isotropic medium yields (Vanelle et al., 2011a):

$$\frac{\partial t}{\partial\theta} = \underbrace{\left(\frac{H}{v_1^2 t_1} + \frac{H}{v_2^2 t_2}\right)}_{A} R\sin\theta + \underbrace{\left(-\frac{x_1 - x_c}{v_1^2 t_1} - \frac{x_2 - x_c}{v_2^2 t_2}\right)}_{B} R\cos\theta. \quad (4)$$

Setting $\partial t/\partial\theta$ to zero leads to the following expression for the tangent of the reflection point angle:

$$\tan\theta = -\frac{B}{A} = \frac{x_1 v_2^2 t_2 + x_2 v_1^2 t_1}{H(v_2^2 t_2 + v_1^2 t_1)} - \frac{x_c}{H}. \tag{5}$$

Switching from source and receiver to midpoint and half-offset coordinates (5) changes to:

$$\tan\theta = \frac{x_m - x_c}{H} - \frac{h(v_2^2 t_2 - v_1^2 t_1)}{H(v_2^2 t_2 + v_1^2 t_1)}. \tag{6}$$

The equation for $\tan\theta$ has to be solved in order to compute the traveltime. Indeed, it depends on the traveltime itself and thus is an implicit formula. However, one can make use of the fact that equations (5) and (6) become explicit for the case of zero offset:

$$\tan\theta_0 = \frac{x_m - x_c}{H}. \tag{7}$$

The computed θ_0 can thus be used as a starting guess of θ for a recursive application, as suggested by Vanelle et al. (2010).

In order to fit into multi-parameter stacking implementations like the CRS stack, the i-CRS operator has to be capable of considering neighboring CMP gathers. Therefore, the absolute source and receiver coordinates as well as the horizontal position of the reflector have to be transformed into relative coordinates with respect to a central location x_0 in the used aperture. This can be achieved by:

$$x_{1,2} - x_c = x_{1,2} - x_0 - x_c + x_0 = \Delta x_{1,2} - \Delta x_c \tag{8}$$

resulting in the final set of equations, which form the new i-CRS multi-parameter stacking operator for converted waves:

$$t = t_1 + t_2 \tag{9a}$$

$$t_1 = \frac{1}{v_1}\sqrt{(\Delta x_1 - \Delta x_c - R\sin\theta)^2 + (H - R\cos\theta)^2} \tag{9b}$$

$$t_2 = \frac{1}{v_2}\sqrt{(\Delta x_2 - \Delta x_c - R\sin\theta)^2 + (H - R\cos\theta)^2} \tag{9c}$$

$$\tan\theta_0 = \frac{\Delta x_m - \Delta x_c}{H} \tag{9d}$$

$$\tan\theta = \frac{v_2^2 t_2 \Delta x_1 + v_1^2 t_1 \Delta x_2}{H(v_2^2 t_2 + v_1^2 t_1)} - \frac{\Delta x_c}{H} \tag{9e}$$

The operator is formulated in source and receiver coordinates here, because this does not imply assumptions about the midpoint location, which is not straightforward in asymmetric settings like converted waves.

PARAMETERIZATIONS

There are several reasons for parameterizing the i-CRS operator in terms of the kinematic wavefield attributes α, R_{NIP} and R_N instead of Δx_c, H and R. First, Δx_c, H and R lose their physical meaning in inhomogeneous media, where they become effective parameters. This applies to $v_{P,S}$ similarly. Second, the i-CRS operator has to be expressed in terms of t_0 and the kinematic wavefield attributes in order to be embedded into current CRS stacking environments. It is also possible to use the operator with its original parameters, but this requires finding a way to incorporate t_0 and designing a new stacking environment. Schwarz (2011) introduced two fundamentally different parameterizations of the i-CRS operator in terms of the CRS attributes, which are presented in the following.

i-CRS3: three-parameter expression

The shifted i-CRS uses an auxiliary medium with constant velocities to describe the traveltime moveout. This is possible because the CRS parameters (α, R_{NIP}, R_N) are characteristics of the reflector recorded at

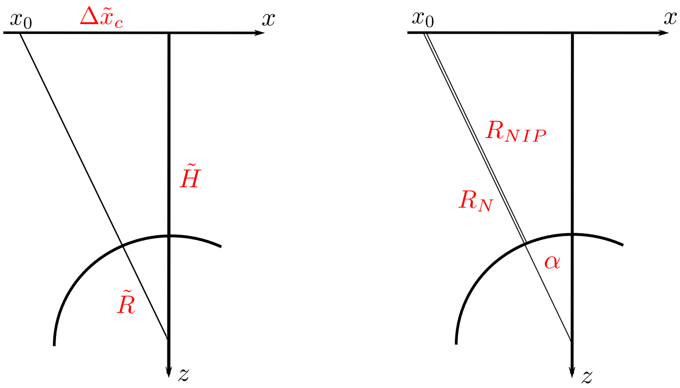

Figure 1: Geometric relations between i-CRS (left) and CRS parameters (right) in a homogeneous medium (Schwarz, 2011).

the surface. Therefore, the description of traveltime moveout can be carried out in a so-called image space (e.g., Höcht et al., 1999) using the constant near-surface velocities. This auxiliary medium leads to simple, geometric relations between i-CRS and CRS parameters (Schwarz, 2011, see also Figure 1):

$$\Delta\tilde{x}_c = -R_N \sin\alpha, \tag{10a}$$
$$\tilde{H} = R_N \cos\alpha, \tag{10b}$$
$$\tilde{R} = R_N - R_{NIP}, \tag{10c}$$
$$\tilde{v}_{P,S} = v^0_{P,S}. \tag{10d}$$

The tilde in the i-CRS parameters indicates that these relations hold for heterogeneous media, i.e., the parameters become effective parameters, whereas the original i-CRS derivation was carried out for the homogeneous case. See also Figure 1 for the geometric relations.

Since traveltime moveouts in image space and model space are supposed to be equal (de Bazelaire, 1988; Höcht et al., 1999), the traveltime can be calculated entirely in the image space before subtracting a constant time shift t_r. This time shift also introduces t_0 and reads:

$$t_r = \frac{2R_{NIP}}{v^+} - t_0, \tag{11}$$

where $2R_{NIP}/v^+$ describes the zero-offset traveltime in the image space, which follows from the geometric relations in Figure 1. The velocity v^+ is the harmonic average of the near-surface P- and S-wave velocities. The traveltime description for the shifted i-CRS finally reads as follows:

$$t_{shift} = t_1(\alpha, R_{NIP}, R_N) + t_2(\alpha, R_{NIP}, R_N) + t_0 - \frac{2R_{NIP}}{v^+}. \tag{12}$$

As this traveltime expression uses three parameters, we refer to it as 'i-CRS3' from here on.

i-CRS5: five-parameter expression

Schwarz (2011) expanded the squared monotypic i-CRS traveltime into its Taylor series and compared the resulting coefficients with the ones of the parabolic CRS formula. Introducing the normal moveout velocity defined as follows,

$$v^2_{NMO} = \frac{2R_{NIP}v^+}{t_0\cos^2\alpha}, \tag{13}$$

this resulted in the following new parameter transformation formulae:

$$\Delta\tilde{x}_c = \frac{-R_N \sin\alpha}{\cos^2\alpha\left(1+\frac{v_{NMO}}{(v^+)^2}\sin^2\alpha\right)}, \tag{14a}$$

$$\tilde{H} = \frac{v^+ R_N}{v_{NMO}\cos^2\alpha\left(1+\frac{v_{NMO}}{(v^+)^2}\sin^2\alpha\right)}, \tag{14b}$$

$$\tilde{R} = \frac{\frac{v^+ R_N}{v_{NMO}\cos^2\alpha} - \frac{v_{NMO}t_0}{2}}{\sqrt{1+\frac{v_{NMO}}{(v^+)^2}\sin^2\alpha}}. \tag{14c}$$

For the case of converted waves, a transformation formula for the velocity $\tilde{V}$ of the same form as the monotypic case,

$$\tilde{V} = \frac{v_{NMO}}{\sqrt{1+\frac{v_{NMO}}{(v^+)^2}\sin^2\alpha}}, \tag{15}$$

can be derived. However, the down- and up-going rays depend on different velocities. Introducing v_1 and v_2, Taylor i-CRS becomes a five parameter (i.e., $\alpha, R_{NIP}, R_N, v_1, v_2$) traveltime description. Because of this, we refer to it as 'i-CRS-5'.The transformation formula for $\tilde{V}$, (15), is therefore not required and the two optimized velocities are directly used for the computation of the traveltime.

In the presence of heterogeneities, the two velocities become effective parameters, just like the original CRS parameters α, R_{NIP}, R_N. In order to distinguish them from the homogeneous case, they will be denoted as $\tilde{V}_P$ and $\tilde{V}_S$ from now on. Additionally, instead of v^+ in (14) we introduce $\tilde{V}_{eff}$ as the harmonic mean of the optimized effective velocities $\tilde{V}_P$ and $\tilde{V}_S$ in the heterogeneous case.

Since the transformation relations (14) already contain the zero-offset traveltime t_0, the traveltime description for this parameterization is a pure double-square root expression, which reads:

$$t_{Taylor} = t_1(t_0, \alpha, R_{NIP}, R_N, \tilde{V}_P) + t_2(t_0, \alpha, R_{NIP}, R_N, \tilde{V}_S). \tag{16}$$

In the following sections, we investigate these two parameterizations with respect to sensitivity and accuracy. For comparison, the accuracy of the simplified CRS expression (1) was also studied.

SENSITIVITY STUDY

In this section, we perform a sensitivity study of the three- and five-parametric operators i-CRS3 and i-CRS5 according to Tygel et al. (2011). The purpose is to establish whether the optimization parameters can be estimated accurately by the operators or, in other words, how strong inaccurate parameters affect the calculated traveltime. The sensitivity study is carried out for the following homogeneous model parameter values:

$$\alpha = 10^\circ \qquad v_P^0 = 2000\ \mathrm{ms}^{-1}$$

$$R_{NIP} = 1000\ \mathrm{m} \qquad v_S^0 = \frac{v_P}{\sqrt{3}}$$

$$R_N = 2000\ \mathrm{m} \qquad t_0 = \frac{2R_{NIP}}{v^+}$$

With these values, reference traveltimes are calculated by the two operators. Then, every single one of the optimization parameters is varied from -10 % to 10 % of its model value in steps of 1 % while the others are kept at their model values. For this set of perturbed values, the traveltime is calculated by the respective operator and compared to the corresponding reference traveltime. This procedure is repeated for all optimization parameters, i.e. the CRS parameters for i-CRS3 and the CRS parameters plus the two velocities for i-CRS5. Figures 2(a) and 2(b) show the operators' sensitivities to the CRS parameters and

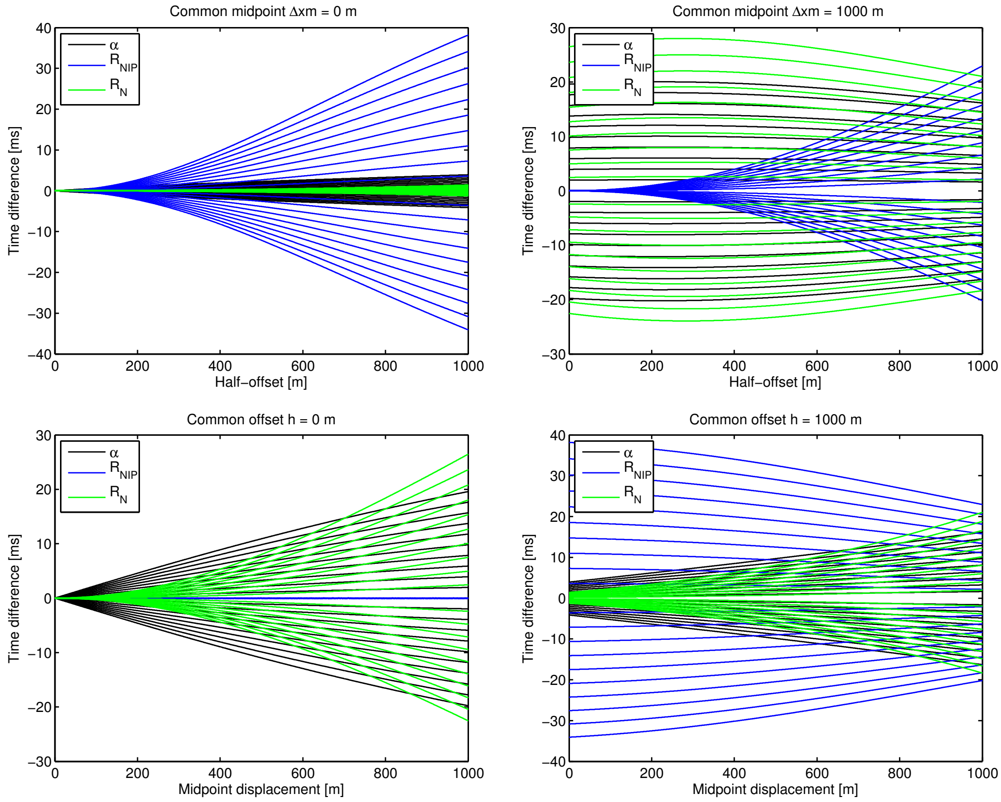

(a) i-CRS3

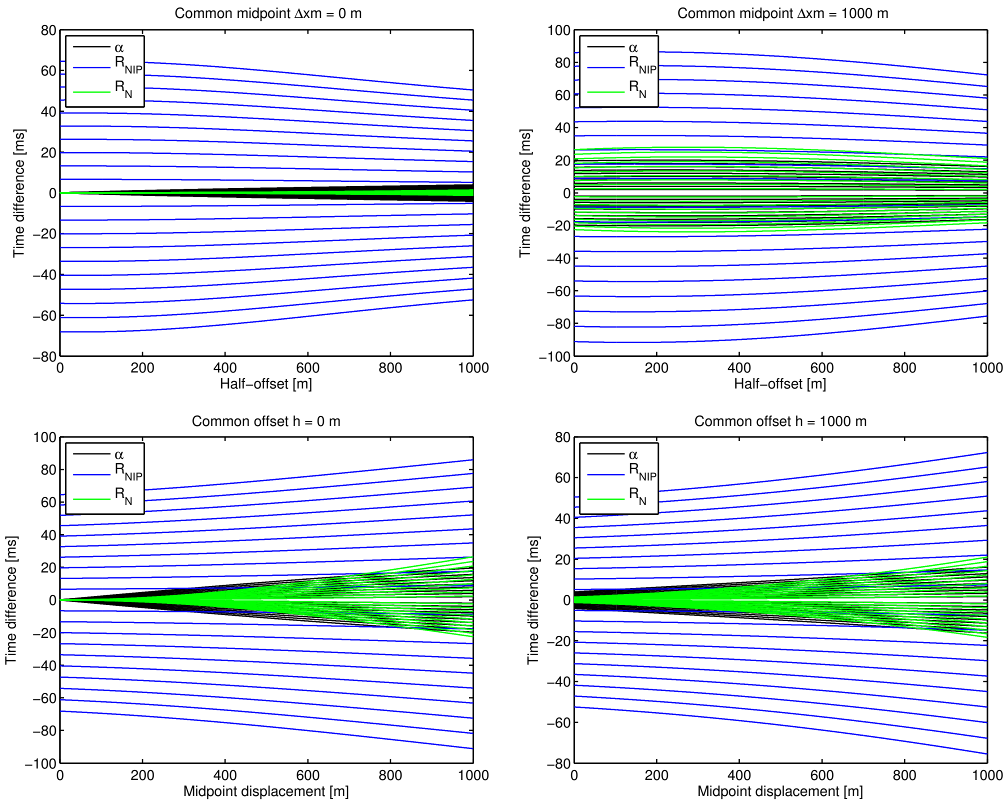

(b) i-CRS5

Figure 2: Sensitivity of the i-CRS operators to CRS attributes

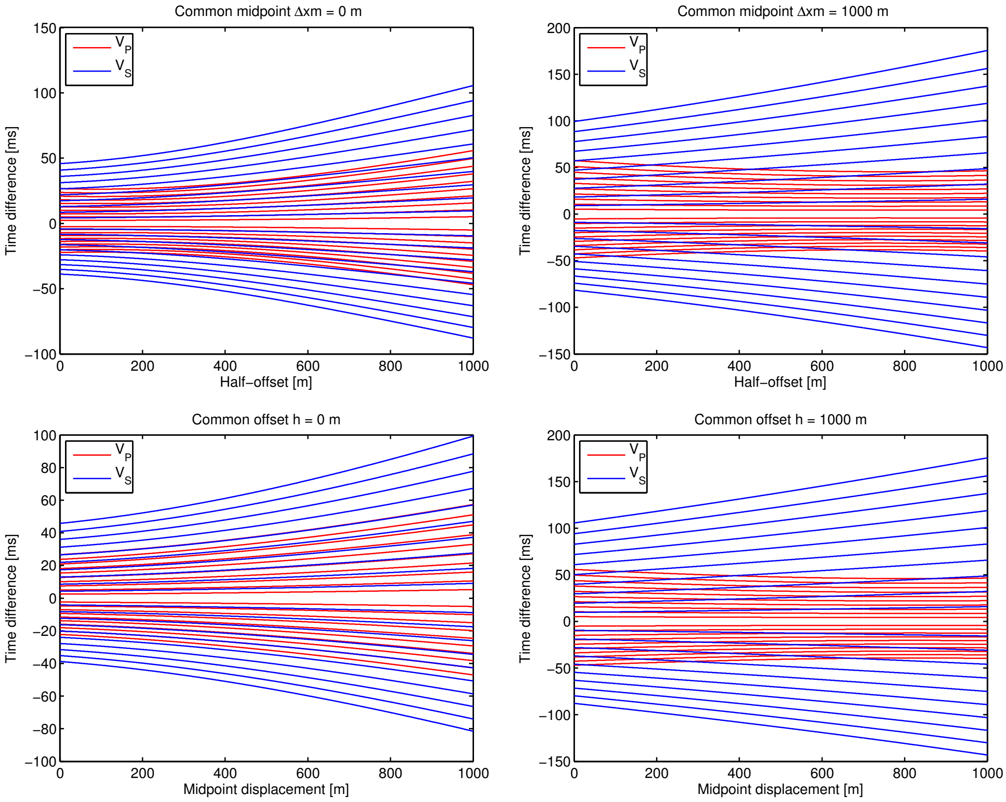

Figure 3: Sensitivity of i-CRS5 to velocities.

Figure 3 shows the i-CRS5 sensitivity to the two velocities.

Whereas both i-CRS3 and i-CRS5 basically have the same sensitivity to α and R_N, they reveal major differences concerning R_{NIP}: over the full $(\Delta x_m, h)$-plane, i-CRS5 is more sensitive to the value of R_{NIP}. In particular, it is also sensitive to R_{NIP} for zero-offset, in contrast to i-CRS3. Both operators are not sensitive to α and R_N for $(\Delta x_m, h) = (0, 0)$. The i-CRS5 operator reveals to be more sensitive to V_S than to V_P, which was to be expected since $V_P > V_S$. We conclude that V_S and R_{NIP} are the two parameters causing the highest traveltime error for i-CRS5 when they are perturbed. The i-CRS3 expression requires large half-offsets for an accurate estimation of R_{NIP}. Furthermore, both operators require large midpoint displacements for an accurate estimation of α and R_N.

ACCURACY STUDIES

In this section, we examine the accuracy of the new traveltime descriptions for simple homogeneous and vertically inhomogeneous models. These models contain circular reflectors with radii of curvature 100 m, 1000 m and 10000 m, whose top point lies in a depth of 1000 m each. The respective position of the reflectors' centers is $\Delta x_c = 0$ (see Figure 4 for a schematic overview of all models in use). Furthermore, we consider three different overburdens for each radius:

1. a homogeneous overburden with constant velocities $v_P^0 = 2000$ m/s and a constant v_P/v_S ratio of $\gamma = \sqrt{3}$,

2. an inhomogeneous overburden with a vertical P-wave velocity gradient of $\partial v_P/\partial z = 0.3\text{s}^{-1}$ starting with $v_P^0 = 2000$ m/s at the surface, and a constant velocity ratio $\gamma = \sqrt{3}$,

3. a vertically inhomogeneous overburden with a vertical P-wave velocity gradient of $\partial v_P/\partial z = 0.3\text{s}^{-1}$

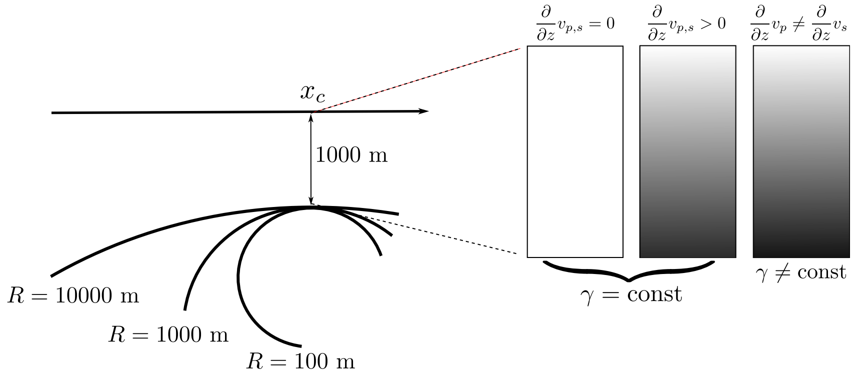

Figure 4: Schematic overview of the different models underlying the accuracy studies. For each reflector radius three different versions of overburden are used (Schwarz (2011), modified).

with $v_P^0 = 2000$ m/s and a vertical S-wave velocity gradient of $\partial v_S/\partial z = 0.4\text{s}^{-1}$ with $v_S^0 = 2000/\sqrt{3}$ m/s.

For this accuracy study we investigate not only the new i-CRS3 and i-CRS5 operators, but also the simplified CRS operator for converted waves (see Equation (1)), which is a hyperbolic three parameter formula.

In the i-CRS implementations, we chose to apply three iterations. The traveltime fits obtained for each operator and model are then compared to the particular exact traveltime, which was computed using the NORSAR 3D software. The following aperture in terms of midpoint and half-offset coordinates was defined in the synthetic data:

$$\Delta x_m \in \{0, 1000\,\text{m}\}, \tag{17a}$$
$$h \in \{0, 1000\,\text{m}\}. \tag{17b}$$

Please note that the sharp edges that are visible in some of the error plots given below are caused by the synthetic data and related to limitations of the ray tracing implementation. Although they appear to be most prominent for the i-CRS5, they are not caused by the operator itself. The reason that they are so pronounced for the i-CRS5 is that the overall accuracy of that operator is higher than for i-CRS3 and CRS. Furthermore, in some of the examples given below, the aperture range (see (17)) is smaller. This is also due to ray tracing issues, which occur here especially for higher reflector curvature.

The operator traveltimes are computed in MATLAB and the parameter optimization is carried out by the intrinsic MATLAB function `fminsearch`, which uses a Nelder-Mead simplex search method (Lagarias et al., 1998). For the traveltime computation, it minimizes the square of the traveltime error.

Example: homogeneous overburden

The results for the homogeneous overburden (see Figure 5 and Table 1) show that the two i-CRS operators lead to consistently higher accuracy than CRS throughout the whole range of reflector curvature. A comparison between the different curvatures reveals that the accuracy of CRS decreases for small reflector radii, i.e., high curvatures. This is not surprising, since the hyperbolic CRS operator is exact for a planar reflector, whereas the non-hyperbolic i-CRS formulas are exact for diffractions. For the homogeneous models, both i-CRS operators reach an accuracy that is basically of the order of machine precision.

The results show the superior performance of the two i-CRS operators over CRS for converted waves concerning not only accuracy, but also parameter estimation (Table 1). All parameter values gained by the optimization procedure are very accurate for both i-CRS3 and i-CRS5, whereas the CRS values show much

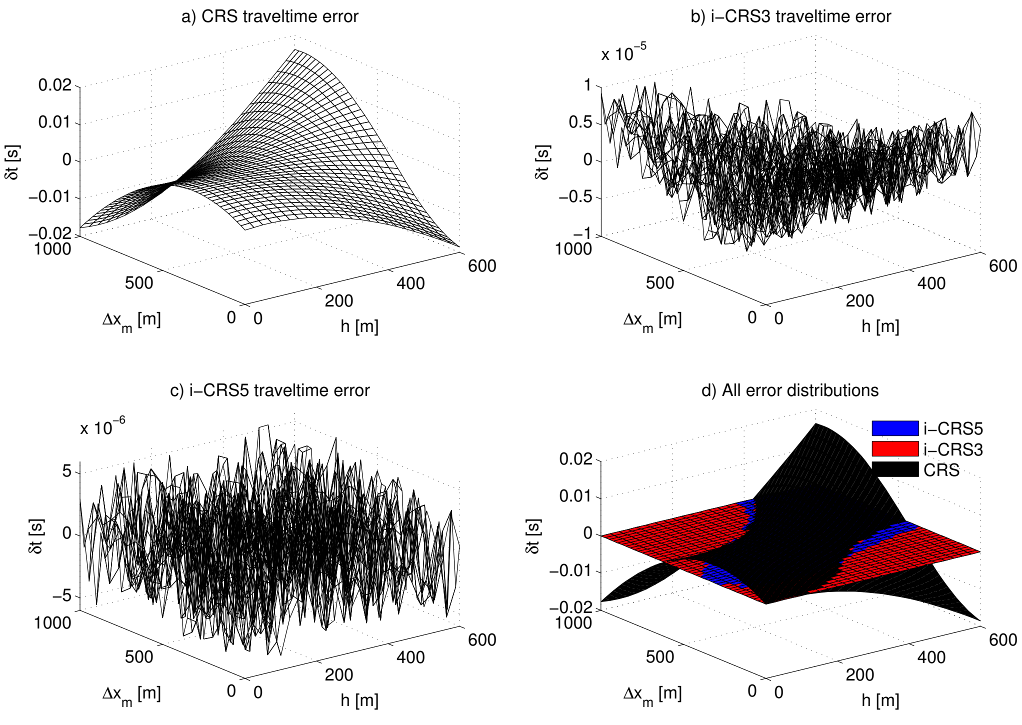

(a) $R = 100\,\text{m}$

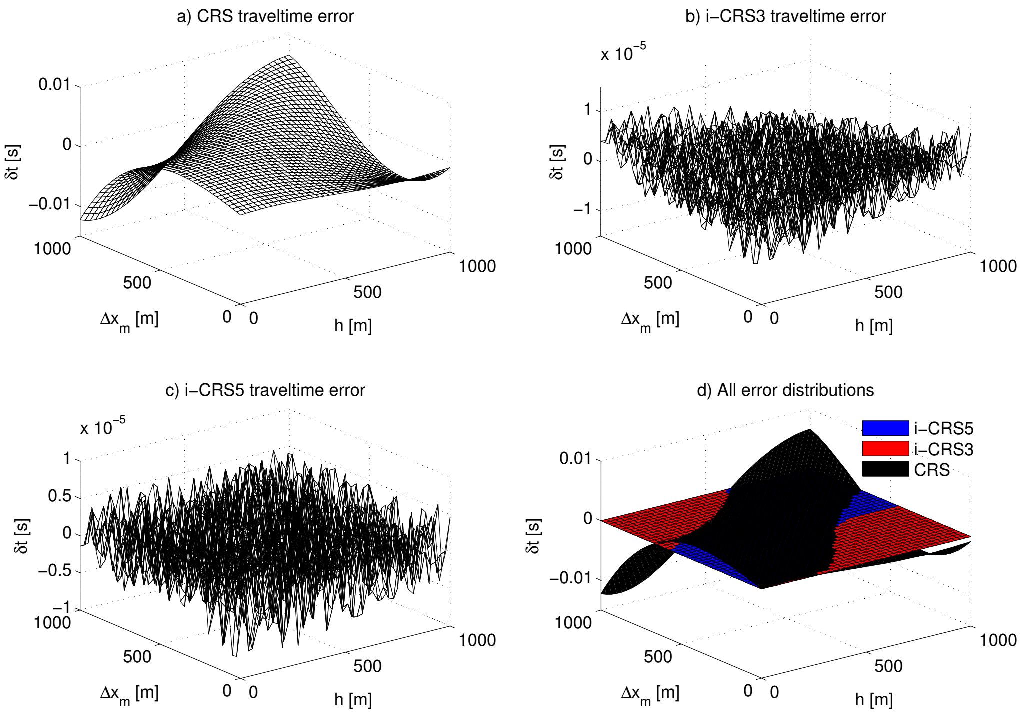

(b) $R = 1000\,\text{m}$

Figure 5: Traveltime errors of the three operators for a circular reflector and a homogeneous overburden. Note the different scales.

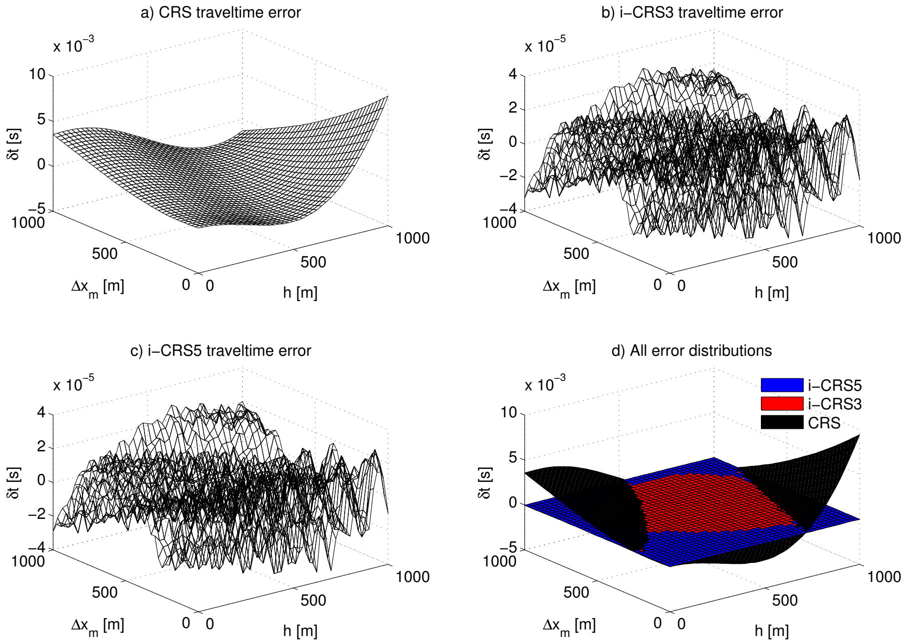

(c) $R = 10000\,\mathrm{m}$

Figure 5: (continued): Traveltime errors of the three operators for a circular reflector and a homogeneous overburden. Note the different scales.

Table 1: Accuracy and estimated parameters for a circular reflector and a homogeneous overburden

(a) $R = 100\,\mathrm{m}$.

	δt_{RMS} [s]	α [°]	R_{NIP} [m]	R_N [m]	V_P [ms^{-1}]	V_S [ms^{-1}]
CRS	$6.602 \cdot 10^{-3}$	1.299	1124.346	1188.187	–	–
i-CRS3	$3.614 \cdot 10^{-6}$	−0.001	999.950	1099.905	–	–
i-CRS5	$2.872 \cdot 10^{-6}$	−0.000	999.999	1099.991	2000.006	1154.660
exact	–	0	1000	1100	2000	1154.668

(b) $R = 1000\,\mathrm{m}$.

	δt_{RMS} [s]	α [°]	R_{NIP} [m]	R_N [m]	V_P [ms^{-1}]	V_S [ms^{-1}]
CRS	$3.207 \cdot 10^{-3}$	0.419	1016.395	2036.167	–	–
i-CRS3	$3.520 \cdot 10^{-6}$	−0.001	999.963	1999.786	–	–
i-CRS5	$3.088 \cdot 10^{-6}$	−0.001	1000.002	1999.944	2000.000	1154.660
exact	–	0	1000	2000	2000	1154.668

(c) $R = 10000\,\mathrm{m}$

	δt_{RMS} [s]	α [°]	R_{NIP} [m]	R_N [m]	V_P [ms^{-1}]	V_S [ms^{-1}]
CRS	$1.895 \cdot 10^{-3}$	−0.060	1027.518	9958.403	–	–
i-CRS3	$1.407 \cdot 10^{-5}$	0.000	1000.015	10997.359	–	–
i-CRS5	$1.394 \cdot 10^{-5}$	−0.001	1000.050	10993.653	1999.913	1154.751
exact	–	0	1000	11000	2000	1154.668

larger deviations and depend on the reflector curvature. For the homogeneous models, the velocity values estimated by both i-CRS operators are very accurate throughout the full range of reflector curvature.

Example: vertically inhomogeneous overburden with constant γ

In this example, we carry out our investigations with the same reflector geometry as before, but with a constant vertical P-velocity gradient of $0.3\,\mathrm{s}^{-1}$ and a constant ratio of P- and S-velocities (γ) instead of a homogeneous overburden. Under these conditions, the operators' behavior reveals larger differences, especially between the two i-CRS implementations.

In terms of traveltime errors, i-CRS5 leads to higher accuracy than the other two operators. As before, the differences decrease for increasing reflector curvature. Whereas the differences in traveltime error between i-CRS3 and i-CRS5 are of the same order in the homogeneous case, in this case they differ by one order of magnitude. CRS provides slightly worse, but comparable results to i-CRS3 with smaller differences for larger radii. Table 2 lists an overview of errors as well as the estimated parameter values. Since the values of the wavefield attributes are not known in the presence of heterogeneity, they are not given as reference. Figure 6 shows the corresponding traveltime error surfaces.

Table 2: Accuracy and estimated parameters for a circular reflector and a vertically inhomogeneous overburden with constant γ.

(a) $R = 100\,\mathrm{m}$.

	δt_{RMS} [s]	α [°]	R_{NIP} [m]	R_N [m]	V_P [ms^{-1}]	V_S [ms^{-1}]
CRS	$4.385 \cdot 10^{-3}$	0.754	1221.058	1249.098	–	–
i-CRS3	$1.290 \cdot 10^{-3}$	0.646	1124.318	1269.811	–	–
i-CRS5	$1.506 \cdot 10^{-4}$	0.148	1000.850	1117.896	2144.592	1243.126

(b) $R = 1000\,\mathrm{m}$.

	δt_{RMS} [s]	α [°]	R_{NIP} [m]	R_N [m]	V_P [ms^{-1}]	V_S [ms^{-1}]
CRS	$2.746 \cdot 10^{-3}$	0.494	1101.528	2305.182	–	–
i-CRS3	$1.921 \cdot 10^{-3}$	0.771	1121.849	2457.380	–	–
i-CRS5	$3.580 \cdot 10^{-4}$	0.302	1003.068	2119.688	2127.294	1254.017

(c) $R = 10000\,\mathrm{m}$

	δt_{RMS} [s]	α [°]	R_{NIP} [m]	R_N [m]	V_P [ms^{-1}]	V_S [ms^{-1}]
CRS	$1.667 \cdot 10^{-3}$	0.061	1112.305	12061.622	–	–
i-CRS3	$1.224 \cdot 10^{-3}$	0.298	1113.582	14427.774	–	–
i-CRS5	$3.004 \cdot 10^{-4}$	0.143	1004.686	12411.427	2144.806	1250.385

Example: vertically inhomogeneous overburden with varying γ

For this last example, we used a model with varying γ, i.e., a P-velocity gradient of $0.3\,\mathrm{s}^{-1}$ and an S-velocity gradient of $0.4\,\mathrm{s}^{-1}$. Note that all operators were derived under the assumption of a constant velocity ratio. Nevertheless, the observed performance is comparable to the constant γ case, however, there are some differences.

The results show that for varying γ i-CRS5 provides the most accurate traveltimes of all three operators: its traveltime error still is by one order of magnitude smaller than the others. i-CRS3 however, performs worse than CRS for $R = 1000\,\mathrm{m}$ and $R = 10000\,\mathrm{m}$. Table 3 shows the estimated parameters and Figure 7 visualizes the corresponding traveltime error surfaces. Since the CRS parameters α, R_N, R_{NIP} imply a one-way process, i.e., constant γ, reference values are not given in Table 3.

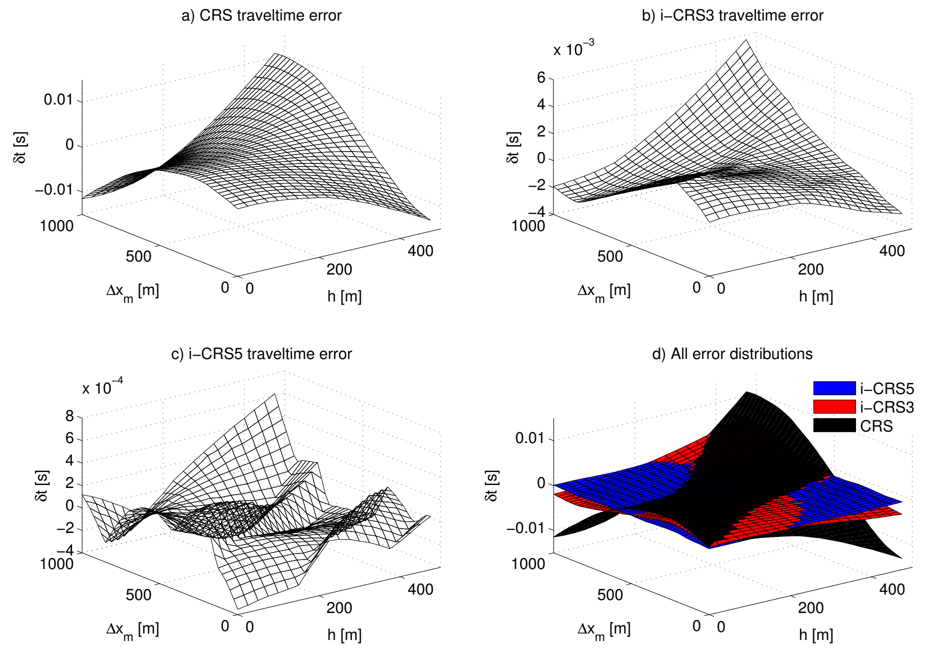

(a) $R = 100\,\mathrm{m}$

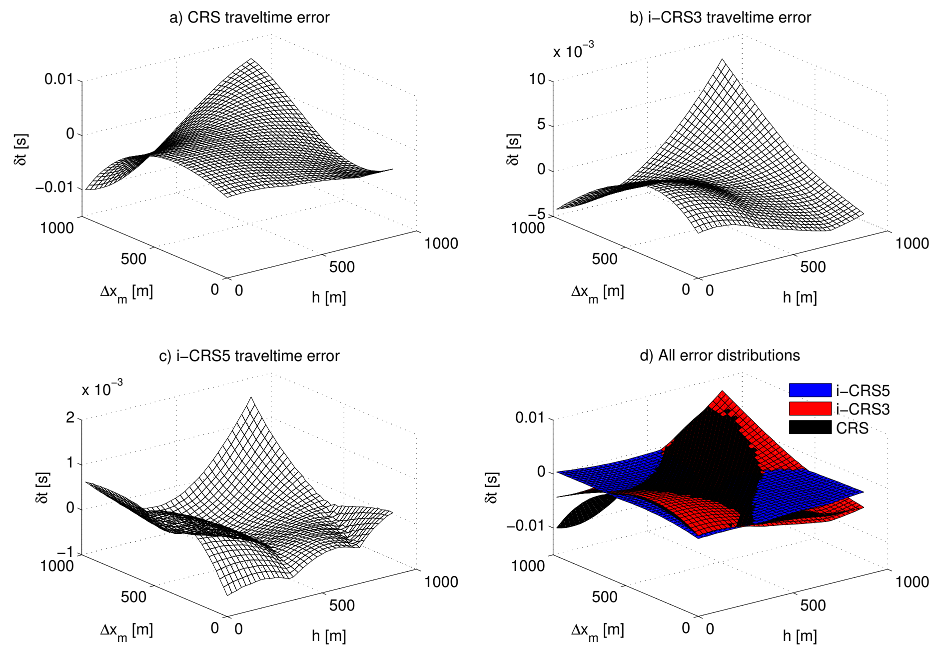

(b) $R = 1000\,\mathrm{m}$

Figure 6: Traveltime errors of the three operators for a circular reflector and a vertically inhomogeneous overburden with constant γ. Note the different scales.

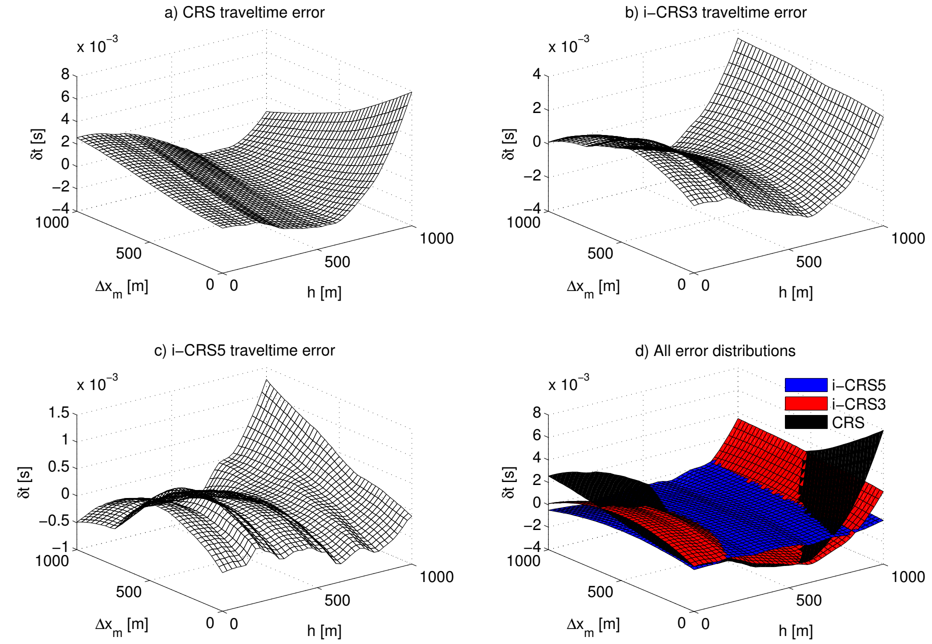

(c) $R = 10000\,\mathrm{m}$

Figure 6: (continued): Traveltime errors of the three operators for a circular reflector and a vertically inhomogeneous overburden with constant γ. Note the different scales.

Table 3: Accuracy and estimated parameters for a circular reflector and a vertically inhomogeneous overburden with variable γ.

(a) $R = 100\,\mathrm{m}$.

	δt_{RMS} [s]	α [°]	R_{NIP} [m]	R_N [m]	V_P [ms^{-1}]	V_S [ms^{-1}]
CRS	$6.078 \cdot 10^{-3}$	1.021	1398.458	1377.464	–	–
i-CRS3	$4.186 \cdot 10^{-3}$	1.296	1325.878	1465.831	–	–
i-CRS5	$3.468 \cdot 10^{-4}$	0.430	1001.765	1142.681	2120.255	1363.198

(b) $R = 1000\,\mathrm{m}$.

	δt_{RMS} [s]	α [°]	R_{NIP} [m]	R_N [m]	V_P [ms^{-1}]	V_S [ms^{-1}]
CRS	$4.721 \cdot 10^{-3}$	1.006	1180.741	2751.752	–	–
i-CRS3	$5.018 \cdot 10^{-3}$	1.620	1235.915	3119.733	–	–
i-CRS5	$7.370 \cdot 10^{-4}$	0.601	1006.706	2223.712	2090.654	1387.245

(c) $R = 10000\,\mathrm{m}$

	δt_{RMS} [s]	α [°]	R_{NIP} [m]	R_N [m]	V_P [ms^{-1}]	V_S [ms^{-1}]
CRS	$1.072 \cdot 10^{-3}$	0.141	1148.219	14512.191	–	–
i-CRS3	$1.457 \cdot 10^{-3}$	0.439	1163.972	18381.997	–	–
i-CRS5	$4.455 \cdot 10^{-4}$	0.204	1008.893	13387.325	2134.598	1370.907

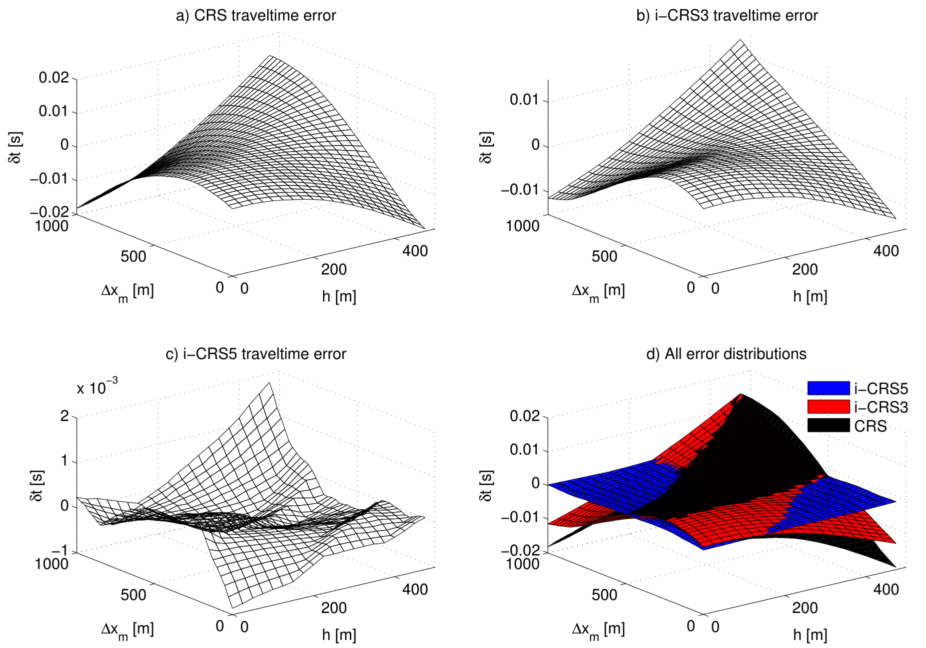

(a) $R = 100\,\mathrm{m}$

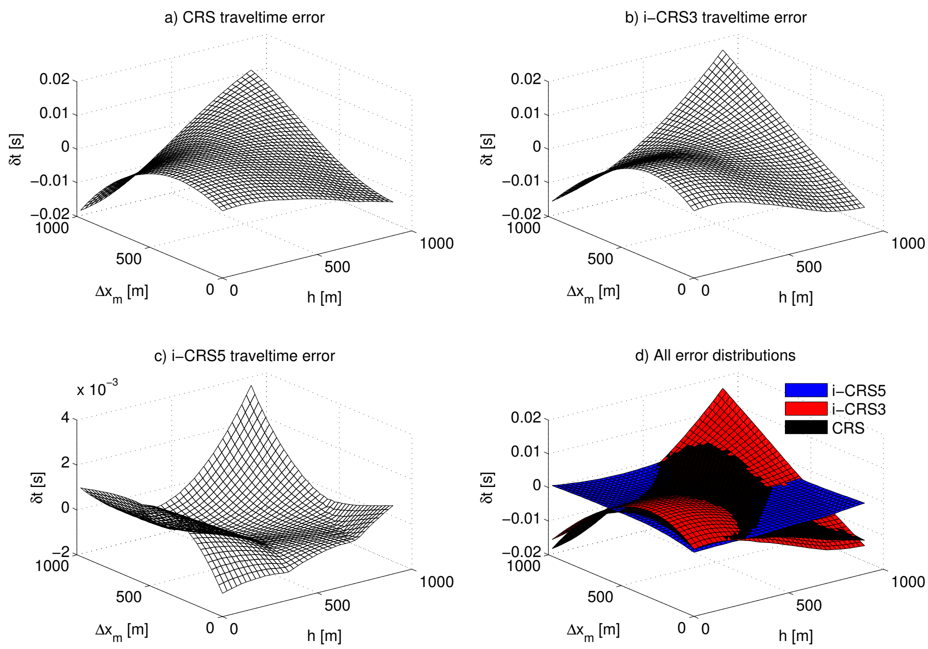

(b) $R = 1000\,\mathrm{m}$

Figure 7: Traveltime errors of the three operators for a circular reflector and a vertically inhomogeneous overburden with variable γ. Note the different scales.

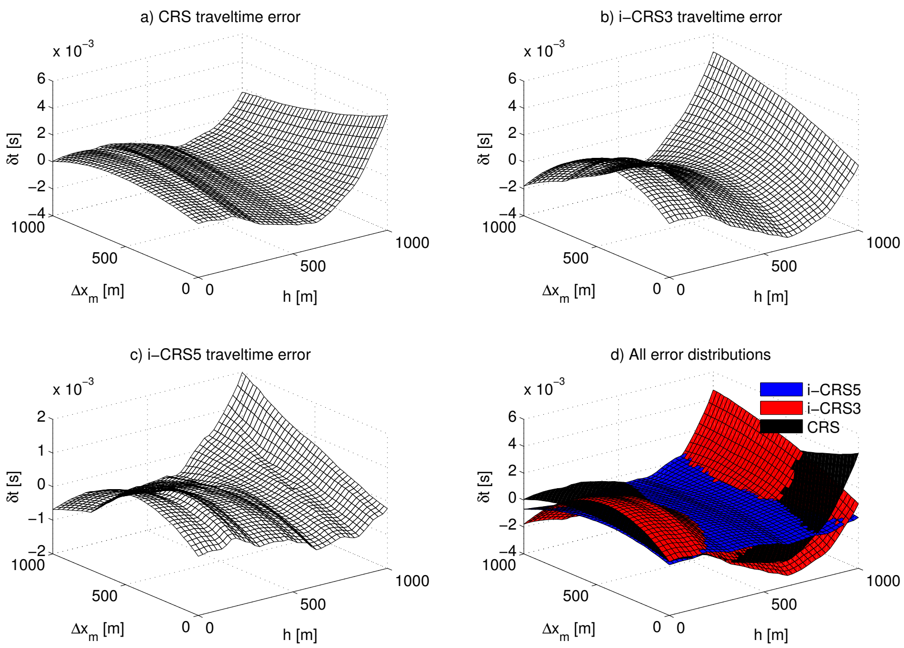

(c) $R = 10000\,\mathrm{m}$

Figure 7: (continued): Traveltime errors of the three operators for a circular reflector and a vertically inhomogeneous overburden with variable γ. Note the different scales.

CONCLUSIONS AND OUTLOOK

In this work, we have investigated the implicit non-hyperbolic traveltime expression, i-CRS, for converted waves based on the work by Vanelle et al. (2011a). Due to its double-square root form, i-CRS has the property of treating the down- and up-going rays separately, which is particularly useful for the case of converted waves, since it allows for the explicit separation of the two velocities.

Two different parameterizations of i-CRS in terms of the CRS attributes, leading to two new traveltime formulations, were examined. In the first, a three-parametric expression denoted i-CRS3, the traveltime is calculated in an auxiliary medium with constant near-surface velocities with a subsequent constant time shift. The second expression, i-CRS5, transforms the CRS attributes following relations obtained by a Taylor series expansion and introduces two additional parameters, namely the velocities of the down- and up-going rays.

We analyzed the sensitivity of both descriptions with respect to parameter determination according to Tygel et al. (2011). Each parameter value was perturbed under controlled conditions. The behavior of the traveltime deviations revealed that i-CRS5 is more sensitive to the estimation of R_{NIP} than i-CRS3, whereas the sensitivities to α and R_N are comparable.

Furthermore, we have examined the accuracy of i-CRS3 and i-CRS5 in comparison to a simplified CRS, i.e., hyperbolic, expression. We have studied circular reflectors with radii varying from the diffraction to near-planar limit with constant velocity and vertical gradient overburden. Again, the i-CRS5 operator performed better than i-CRS3 and CRS, in particular for high reflector curvatures. In an additional test with constant vertical gradients but varying V_P/V_S ratio, i-CRS5 also led to superior results than i-CRS3 and CRS. This last example is very promising because the derivation of the i-CRS as well as the simplified CRS operator investigated here are based on the assumption of constant γ.

First tests with i-CRS3 implemented into a CRS stacking framework for converted waves provided very promising results compared to other operators (see Bauer, 2012). However, similar tests with the i-CRS5 showed that apparently this operator requires a more faster, more stable and more rapidly converging optimization method than Nelder-Mead. One possibility of such an optimization method could be based on a hybrid method using conjugate direction schemes, as suggested by Minarto and Gajewski (2011). According to our studies, we would then expect that i-CRS5 should lead to even better stacking results than i-CRS3.

Another issue that needs to be addressed for the application as a stacking operator is that stacking of converted-wave data cannot take place in the CMP domain. Instead, the data need to be sorted into common conversion point (CCP) gathers (for conventional stacking, see, e.g., Tessmer et al., 1990). An extension of CCP-stacking for multi-parameter operators has recently been introduced by Abakumov et al. (2011). The authors of that work suggest sorting into γ-CMP coordinates. Just like CCP sorting, however, this process requires a priori knowledge of the v_P/v_S ratio. One possible solution to this problem would be to carry out the entire stacking process for converted waves in source and receiver coordinates. Although Dümmong (2005) has shown that for monotypic waves, this approach is less convincing than the 'classical' CRS stack in midpoint and half-offset coordinates, it might lead to a better performance if converted waves are considered.

ACKNOWLEDGMENTS

We thank the Applied Seismics group in Hamburg, and Ivan Abakumov and Boris Kashtan for continuous discussion. The NORSAR 3D software was used to generate reference traveltimes and MATLAB for the performance studies. This work was kindly supported by the sponsors of the Wave Inversion Technology (WIT) Consortium.

REFERENCES

Abakumov, I., Schwarz, B., Kashtan, B., Vanelle, C., and Gajewski, D. (2011). Double-square root traveltime approximation for converted waves. *15th Annual WIT Report*, pages 15–24.

Bauer, A. (2012). Investigations on a new multi-parameter stacking operator for converted waves. B.Sc. thesis, University of Hamburg.

Bergler, S., Duveneck, E., Höcht, G., Zhang, Y., and Hubral, P. (2002). Common-reflection-surface stack for converted waves. *Stud. geophys. geod.*, 46:165–175.

de Bazelaire, E. (1988). Normal moveout revisited – inhomogeneous media and curved interfaces. *Geophysics*, 52:143–157.

Dümmong, S. (2005). Alternative Implementation des Common Reflection Surface Stapelverfahrens. Diploma thesis, University of Hamburg.

Höcht, G., de Bazelaire, E., Majer, P., and Hubral, P. (1999). Seismics and optics: hyperbolae and curvatures. *Geophysics*, 42:261–281.

Hubral, P. (1983). Computing true amplitude reflections in a laterally inhomogeneous earth. *Geophysics*, 48:1051–1062.

Lagarias, J., Reeds, J. A., Wright, M. H., and Wright, P. E. (1998). Convergence properties of the Nelder-Mead simplex method in low dimensions. *SIAM Journal of Optimization*, 9(1):112–147.

Minarto, E. and Gajewski, D. (2011). Optimization of Common Reflection Surface (CRS) attributes based on a hybrid method. *15th Annual WIT Report*, pages 325–332.

Müller, T. (1999). *The Common Reflection Surface stack method – Seismic imaging without explicit knowledge of the velocity model*. PhD thesis, University of Karlsruhe.

Schwarz, B. (2011). A new nonhyperbolic multi-parameter stacking operator. Diploma thesis, University of Hamburg.

Tessmer, G., Krajewski, P., Fertig, J., and Behle, A. (1990). Processing of PS-reflection data applying a common conversion-point stacking technique. *Geophysical Prospecting*, 38:267–286.

Tygel, M., Perroud, H., Lopes, R., and Krummenauer, R. (2011). Sensitivity analysis of the non-hyperbolic common reflection surface. *15th Annual WIT Report*, pages 333–342.

Vanelle, C., Bobsin, M., Schemmert, P., Kashtan, B., and Gajewski, D. (2011a). RSO: a new multiparameter stacking operator for an/isotropic media. *15th Annual WIT Report*, pages 173–178.

Vanelle, C., Kashtan, B., Abakumov, I., and Gajewski, D. (2011b). A CRS-type stacking operator for converted waves. *15th Annual WIT Report*, pages 179–187.

Vanelle, C., Kashtan, B., Dell, S., and Gajewski, D. (2010). A new stacking operator fur curved subsurface structures. *14th Annual WIT Report*, pages 247–253.